Observational Studies of High Mass Star Formation

August 2026

E. L. Hulsen

Abstract

This study investigates the properties of high mass star formation by searching for variability (significant change in luminosity over a period of time) in massive star forming regions, and linking this variability with the accretion burst phenomenon. A collection of protostar sources observed and imaged by the Atacama Large Millimetre/sub-millimetre Array (ALMA) telescopes are organised into fields containing some sources that have been identified as having continuum variability. Spectral graphs, moment maps, and subtraction moment maps are used to analyse variability in emission lines by investigating the nature of emission from specific outburst tracer chemicals. This study found that bright, line rich sources that had variability in their continuum had the most convincing variability in their chemical lines, and therefore are the most promising sources for further investigation into accretion bursts.

University of St Andrews | FOUNDED 1413

LAIDLAW SCHOLARS

1 Introduction

1.1 What is high mass star formation?

Young, lower mass stars experience accretion bursts, which are periods of rapid mass gain of the protostar; the protostar grows suddenly for a period of time, then slows down, this is one of the processes by which a star forms. This corresponds to episodic increases in luminosity, which can be observed with infra-red telescopes. These accretion bursts were first observed in high mass protostars in 2017 [2]. By studying them we hope to be able to further characterise star formation.

1.2 The data

The data for this project came from the Atacama Large Millimetre/sub-millimetre Array (ALMA) which is an interferometer of 66 telescopes in the Atacama Desert, Chile, that measure millimetre and sub-millimetre (infrared) wavelengths of radiation. The ALMAGAL survey used ALMA to build a database of star forming regions throughout the galaxy (among other things), which have been used in countless research projects and explorations of this field.

During COVID-19, there was a break in data collection, which conveniently allows us to compare the luminosity flux data with a gap of a few years in between. By comparing the luminosity of these massive young stellar objects between December 2019 and March 2022, it is possible to observe variability in the sources; that is changes of luminosity due to accretion bursts.

1.3 How do we measure and observe accretion bursts?

Accretion bursts are seen when the continuum (overall luminosity of the source) changes over time. Examples of significant changes in continuum luminosity have been observed in some high mass young stellar objects [1]. We can observe this change of luminosity in the spectrum of the source, and this also shows the chemicals present around the source in the form of peaks/lines present in the spectrum at certain frequencies.

An emission spectrum is a way to get information like chemical content and radial velocity of the gas around a source using the light coming from it. Simply explained: when a source radiates energy it excites the electrons in the surrounding gas. Electrons are quantised, meaning they can only gain and lose energy in very specific amounts that will correspond to the chemical structure they are in. After becoming excited, the electron will "drop back down" to its original energy level by emitting a particular frequency of light. Given the presence of clouds of gas containing many of the same molecules, this frequency of emitted light becomes very bright and presents as a large peak in the emission spectrum for that source. By observing the peaks in a source's emission spectrum we can identify the peaks and work out the chemical composition of the surrounding gas clouds.

The changes of the brightness of the chemical lines over time on the emission spectra indicates an accretion burst, and the often organic molecules that do this are called outburst tracers [6].

1.4 Aims of this study

The MYSOs (Massive Young Stellar Objects) are sources organised into fields that each contain 3 or 4 of them. This project investigates 5 of the fields that have been selected by Claudia Cyganowski and Rodrigo H. Alvarez-Gutierrez as containing at least one source that shows variability in its continuum (overall luminosity) and is therefore an accretion burst candidate.

This study will investigate whether the sources (both burst candidates and not) in these fields show variability in their spectral lines, e.g. whether there are luminosity changes in the peaks of specific chemicals. Additionally, moment maps will be used to gain further information about the sources with the aim of finding sources that have clear variability and therefore can be used to study accretion bursts.

This follows a similar analysis to [5] by using multiple epochs (dates) comparatively and moment maps, to observe variability in the sources.

1.5 Key terms

ALMA - Atacama Large Millimetre/sub-millimetre Array, the collection of telescopes in Chile that collected the data.
MYSOs or sources - Massive Young Stellar Objects, the high mass protostars (sources) that this project is investigating.

CASA - Common Astronomy Software Application, the software used to view and manipulate the data collected by ALMA.
Spectral plot - a graph that shows the emission spectra of a source at different dates (epochs).
Moment map - a "map" showing where the emission of certain chemicals is coming from in the field.
Continuum - the data that shows the overall luminosity (and change in that luminosity over time) of a source.
Spw - Spectral Window, this refers to a specific range of frequencies, so each source will have multiple spectral graphs to cover every spw.

2 Methods

Throughout this project, the Common Astronomy Software Applications (CASA) package was used to process the data, and produce the spectral graphs and moment maps.

2.1 Notes on the data

The data used was stored as convolved beam cubes, which means each image of a field at a particular epoch had many channels that corresponded to a range of frequencies. "Convolved" means that the images are all able to be compared, as they have a similar angular resolution (1"~2"). The convolved beam is important to the process of producing the spectra, as it allows the fluxes of the various epochs to be compared, which is crucial for identifying variability.

This study analyses 5 fields (50555, 53869, 56184, 57335, 58516), each of which contains 3-4 sources, which were labelled MM1, MM2 etc. in order of luminosity. In every field, MM1 was the source previously identified as having continuum variability. Images of all the fields and their constituent sources can be found in Appendix C.

There were three epochs, 17th December 2019, and 28th and 29th March 2022. The ~2.3 year difference between the December 2019 date and March 2022 dates allows us to look for variability, whereas the two March 2022 dates are expected to match, and can be used to evaluate how convincing the variability is.

There were 4 spws, two narrow (29,31) and two broad band (25,27). The narrow band spws had much higher resolution and therefore provide more convincing evidence regarding whether there is variability in the spectra or not. Whilst the broad band spws have lower resolution, they cover a wider range of frequencies and therefore contain more spectral lines. As seen in Figure 1, spw 29 (2) is part of spw 25 (0), and spw 31 (3) is part of spw 27 (1).

When chemicals are referenced in Table 1, Table 3, and the main text of this paper, some will have Roman numerals in parenthesis following the chemical formula. This is used to differentiate different lines/frequencies that correspond to the same chemical within a larger spw window (spw 25 and 27). For example CH3OH(III) is the third CH3OH line in spw 25, which also happens to be in spw 29, as seen in Figure 1 below.

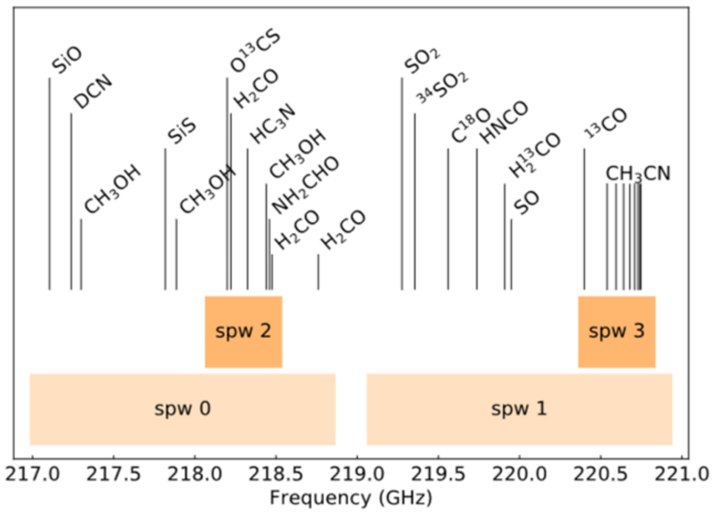

Figure 1: Diagram showing the frequency ranges of the spws, where 0 is spw 25, 1 is spw 27, 2 is spw 29, and 3 is spw 31. Also includes some expected chemical lines. Diagram sourced from [4] (Sanchez-Monge et al., 2025).

2.2 Spectral graphs

2.2.1 Extracting the spectra

The spectral data was extracted for each MMX source in each field, for each epoch and spw range, varying with frequency. The brightest pixel in each source was selected manually, and then a python script written by Rodrigo Hernan Alvarez Gutierrez was used to generate the data files showing how luminosity varies with frequency. This python script included the command `tt.ispec`, which comes from the `toddTools.py` program made by Todd Hunter (link to website here).

2.2.2 Noise measurements

To calculate an error for the luminosity measurements, the background noise was measured. First, regions were drawn for each field. As can be seen in Figure 2, these regions were drawn to avoid picking up emission from the sources, but to have approximately the same radial distance from the centre as them. The noise for each field and epoch (changing with frequency) were then generated using the `rmsfinder` command.

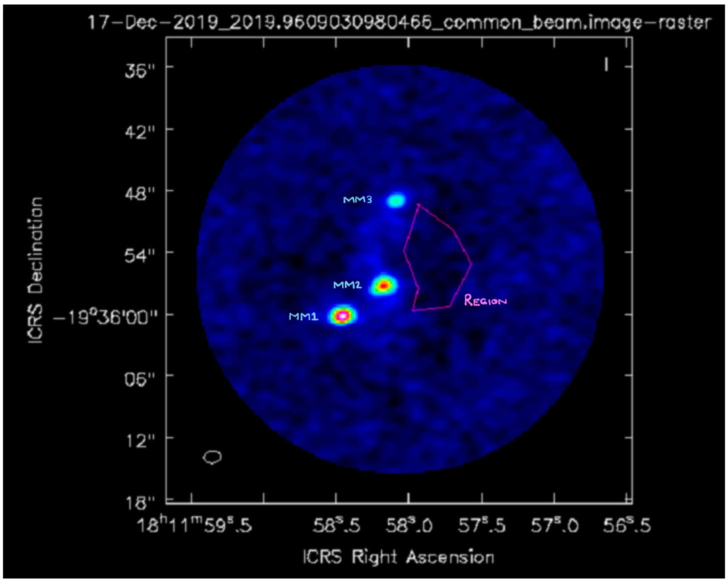

Figure 2: Raster image of field 50555's continuum, with 50555's region over-layered.

2.2.3 Generating the plots

I generated the plots using a python script written by David Taylor (and edited by me to include a correction for the red-shifted peaks, and to change some of the layout). There is a plot for each source and each spw, as they combine epochs in order to compare the peaks.

Each graph contains 3 dashed lines of 4σ (where σ is mean background noise), one for each epoch, along with the noise (σ) measurement for each epoch written in the top left hand corner. This is demonstrated in Figure 3. A peak that is higher than ~4σ, is considered significant enough to identify. The spectra in Figure 3 is considered line rich; meaning it has several significant peaks. Each line is surrounded by a shaded area above and below the line which corresponds to the background noise for that frequency.

2.3 Moment maps

A moment map is used as a representation of the presence of chemicals in and around the sources. It allows us to find out where emission of a particular frequency (corresponding to a particular chemical line) is coming from within the field, and how strong that presence is.

`Casaviewer` (part of CASA software) was used to select the range of channels (corresponding to a narrow range of frequencies) needed for a certain chemical line. Moment 0 and moment 8 maps were then generated using a python script written by Rodrigo Hernan Alvarez Gutierrez. A moment 0 map sums the intensity at every pixel over the channel range, whereas a moment 8 map selects the maximum intensity over the channel range.

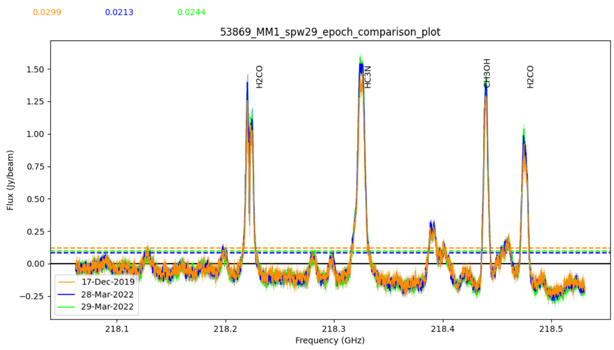

Figure 3: Example of a spectral graph (field: 53869, source: MM1, spw 29), showing σ values, and 4σ dashed lines, this source is considered line rich.

A moment map (of both types) was generated for the chemicals lines H2CO(I), HC3N, and CH3OH(III) for each field and each epoch. These chemical lines (all in spw29) were chosen as they consistently appear in multiple fields. The three (one for each epoch) moment maps for a given chemical line in a given field were all set at the same brightness scaling so they might be compared. A contour map of the continuum image was layered over the moment maps to show where the sources are in the field. An example of a moment map: the CH3OH(III) line, in field 53869, for epoch 17th Dec 2019, can be seen in Figure 4.

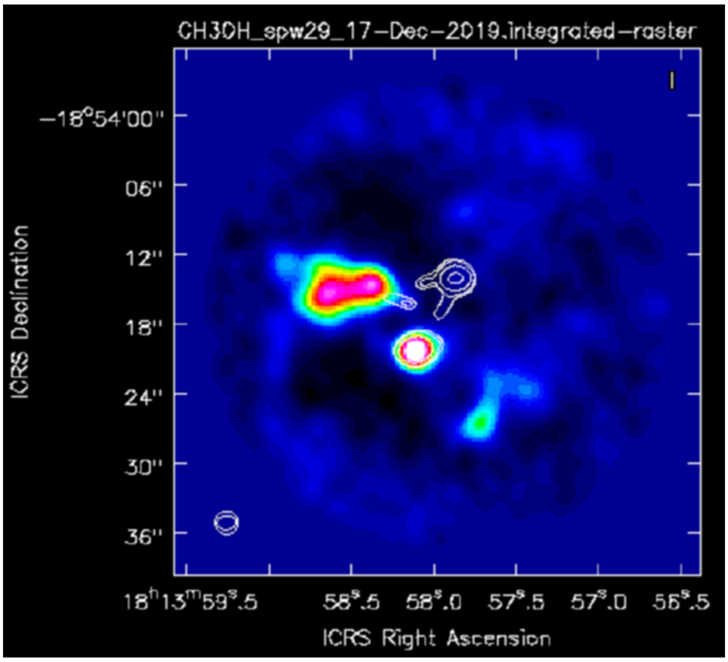

Figure 4: Example of an integrated (moment 0) map (field: 53869, line: CH3OH(III), channel range: 3040 3140, epoch: 17th Dec 2019) with contours of the continuum image overlaid.

2.4 Subtraction moment maps

Subtraction moment maps are maps showing the difference between two epochs by subtracting one moment map from another using a CASA function called `immath`. They are particularly useful to qualitatively observe how and where emission has changed over time.

Only the moment 0 maps were subtracted, due to their greater range of brightness, and therefore clearer differences between brighter and dimmer times or places. There are three subtraction moment maps for each chemical line in each field. As with the ordinary moment maps, a contour map of the continuum image was layered over the images to show where the sources are in the field. An example of a subtraction moment maps: the H2CO(I) line, in field 50555, for epoch difference 28th Mar 2022 - 17th Dec 2019 can be seen in Figure 5.

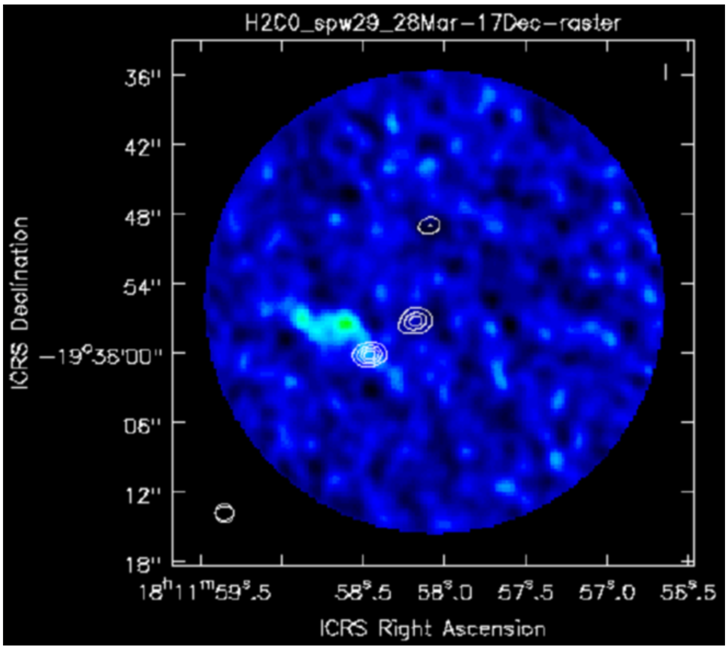

Figure 5: Example of a subtraction moment map (field: 50555, line: H2CO(I), epoch difference: 28th Mar 2022 - 17th Dec 2019) with contours of the continuum image overlaid.

3 Analysis

It was necessary to combine information about the spectral graphs and moment maps of each source, in each field, in a way that enabled various sources and fields to be compared. The tables Table 1 and Table 3 in the appendices, compile this information.

3.1 Spectral graphs analysis

The variability present in spectral graphs relies on the visible difference in luminosity between the December 2019 and March 2022 measurements for a specific chemical line, such that the noise measurements do not overlap. It was much easier to see these differences in sources with strong emission lines significantly higher than the ~4σ line, as weaker sources had greater overlapping background noise measurements. This can be seen in the difference between Sub-figure 6a and Sub-figure 6b in Figure 6 below.

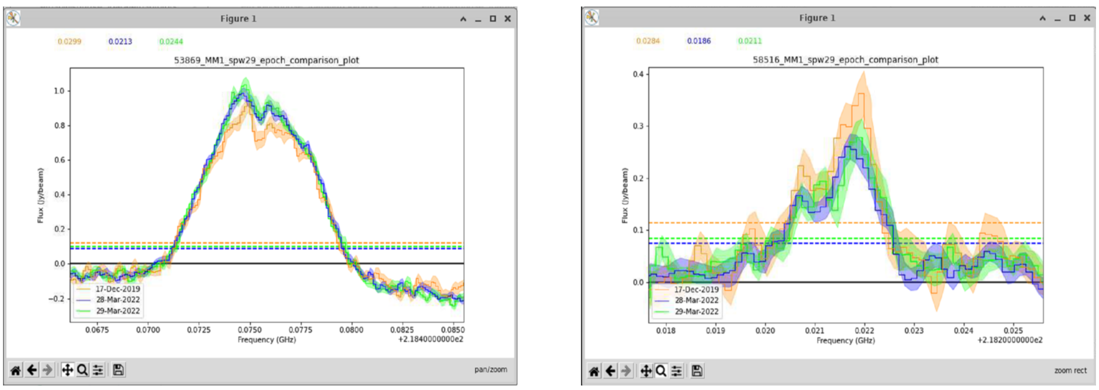

(a) Clear variability (field: 53869, source: MM1, spw 29, line: H2CO(I))

(b) Unclear variability (field: 57335, source: MM1, spw 29, line: H2CO(II))

Figure 6: Comparing evidence of variability.

Some variability was found in the continuum variable source (MM1) for every field apart from 56184, which has no variability at all. Variability is also found in chemical lines for MM2 for several fields, and line rich sources (MM1 in fields 53869 and 57335) are particularly clear and promising. These are all the more luminous sources, with taller peaks and clearer spectral graphs, which might be contributing to more evident variability. Sources that do not have any variable chemical lines tend to have had weaker lines overall. All variability information gained from spectral graphs is summarised in Table 1.

3.1.1 Carbon monoxide

Both CO[13] and CO[18] (two isotopes of carbon monoxide), are cold gas tracers, which means they follow patterns of cold gas that exist around the sources. They are unsuited to being used as any indicator of variability, due to the combination of: the chaotic nature of the line (shown in Figure 7 below), the cold gas not tracing the contours of the sources, and the ALMA telescopes being unable to measure the sudden changes in brightness coming from CO emission. Therefore, all CO line emission in Table 1 is ignored.

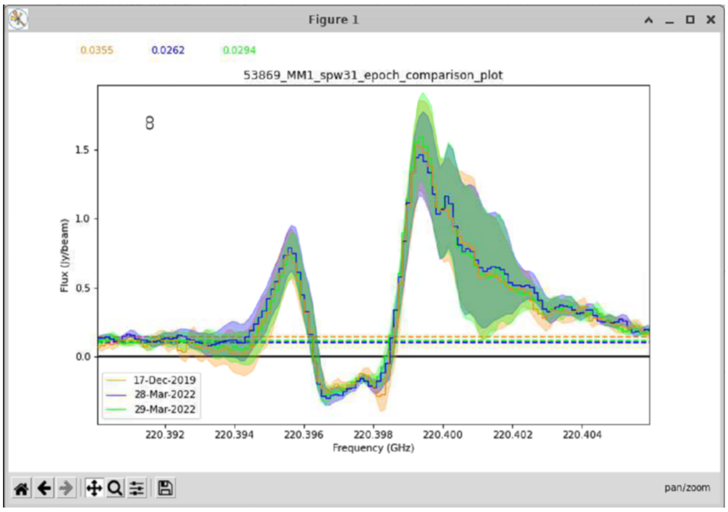

Figure 7: Example of CO 'line' (field: 50555, source: MM1, spw 31, line: CO[13])

3.1.2 Additional graph notes

The spw 29 lines that were identified as variable were also variable when present in spw 25, but it was much harder to judge variability, especially with borderline cases. The same is true of variable spw 31 lines that are present in spw 27. Variability is more convincing if found in spw 29 and 31 because of their greater detail, but also easier to distinguish in these windows.

The graphs of line rich sources present a calibration error wherein the baseline of the graph (expected at y=0) is below the x-axis, especially at higher frequencies. Although this would need to be corrected for detailed numerical analysis of these graphs, it doesn't interfere with the identification of chemical lines and their variability.

In some cases, it was difficult to identify a line with CASA and `casaviewer`, as two possible chemicals exist, whose lines are very close together. This uncertainty has been indicated in Table 1.

3.2 Moment maps analysis

Moment maps were not made for every chemical experiencing variability, but for chemicals that consistently appeared in almost all fields (H2CO(I), HC3N, CH3OH(III)). Compiled descriptions of all moment maps can be found in Table 3. They tell us where a chemical is present in the field, which can reveal more information about the accretion bursts. Some maps show gas clouds centred around the sources, implying that the variability information we gain from that chemical line corresponds to accretion burst activity from the source (Sub-figure 8a). However, many maps show outflows that are either in a different part of the field, or cover sources but are not centred on them (Sub-figure 8b).

The subtraction maps help to re-affirm variability observed in the spectra; a difference in brightness between March 2022 and December 2019 epochs, but not between the consecutive March 2022 dates, indicates reliable variability. This is demonstrated in Figure 9 below.

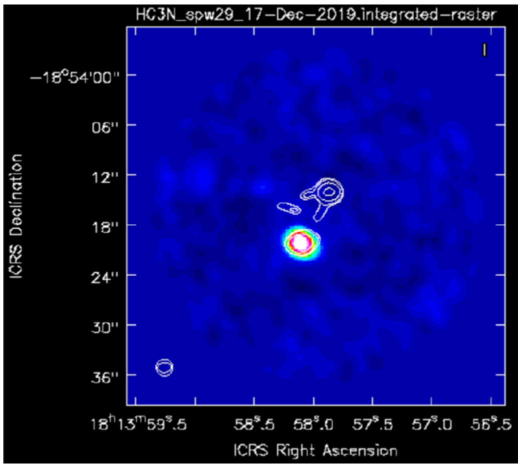

(a) A moment map showing emission centred on a source (field: 53869, line: HC3N, epoch: 17th Dec 2019, type: moment 0 integrated)

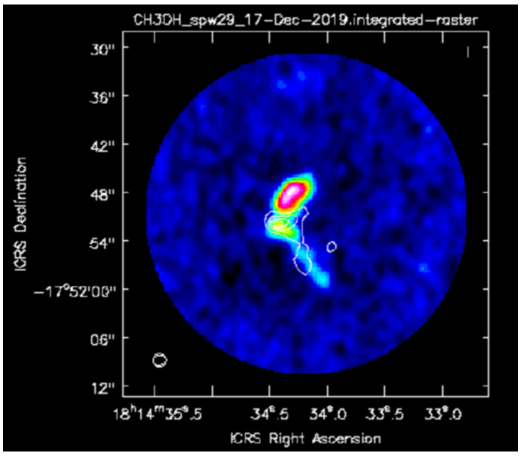

(b) A moment map showing emission coming from an outflow (field: 58516, line: CH3OH(III), epoch: 17th Dec 2019, type: moment 0 integrated)

Figure 8: Comparing emission coming from the protostar source or an outflow.

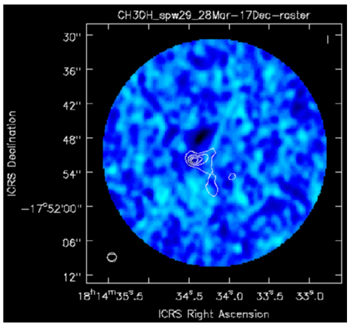

(a) Epoch difference: 28th Mar 2022 - 17th Dec 2019, showing variability.

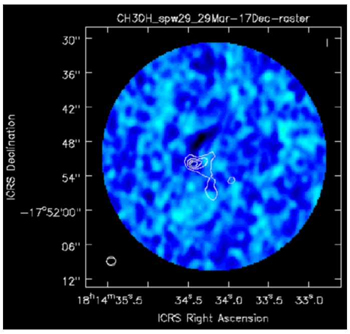

(b) Epoch difference: 29th Mar 2022 - 17th Dec 2019, showing variability.

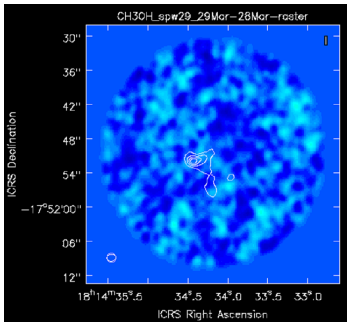

(c) Epoch difference: 29th Mar 2022 - 28th Mar 2022, no variability.

Figure 9: Showing how subtraction moment maps can be used to confirm variability (field: 58516, line: CH3OH).

3.2.1 Outflows

Outflows are streams of material ejected from the core of a source during the early stages of star formation [3]. They also include the chemicals present in the sources, so appear on moment maps as shown in Sub-figure 9b. Although they do reveal information about the formation of a high mass star and the activity of the protostar, they are not directly relevant to this study, which is focused on extracting information about the emission of the sources themselves.

Therefore, outflows are noted in Table 3 but not considered a helpful part of the moment map or subtraction moment map analysis. Emission clearly coming from an MMX source within a field is a condition within the process of selecting the most promising sources.

3.3 Promising sources

As shown in Figure 10, the spectral graphs, moments maps and subtraction moment maps can be combined in such a way to slowly eliminate sources in the fields to identify the most promising for future studies on accretion bursts. After all 4 processes, the two sources left (53869 MM1, 57335 MM1) are the two line-rich sources, both previously identified as having variability in their continuum.

However, any sources showing variability in their spectra (the 7 sources in box 2 of Figure 10) could be useful for further studies into line variability indicating accretion bursts.

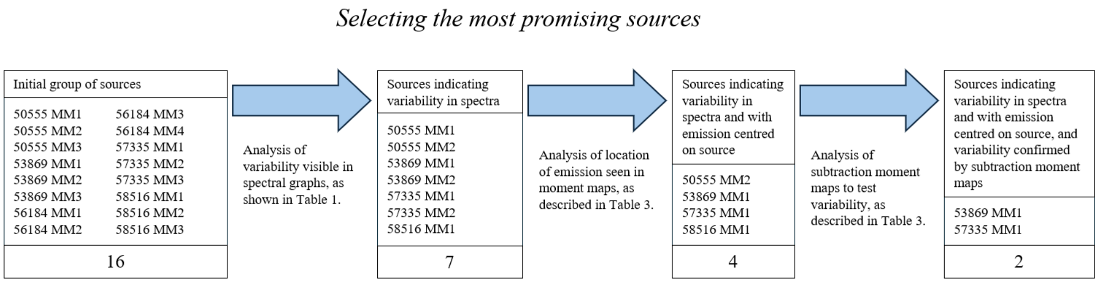

Figure 10: Graphic showing the process of selecting protostars as promising sources of variability.

4 Conclusions and future studies

This study has found that the brightest and most line-rich protostars are the most promising sources of variability, which in turn indicates that they are the most likely to be useful for studying accretion bursts. The methods (spectral graphs and moment maps) used in this study allows for a thorough examination of the light emitted from the sources; building up a full picture of the way they behave and their properties as they pertain to variability. The identification of variable sources contributes to ongoing work in the field of high mass star formation, as more is discovered about the mechanisms that drive it.

This research is the first step in what will hopefully be a much wider exploration of protostar accretion bursts using ALMA data. Future studies could:

- perform similar analysis on a wider range of sources.
- produce more detailed spectral graphs (e.g. for the parts of spw 25 and 27 which are not covered by spw 29 and 31), in order to be able to conclude more decisively regarding variability in chemical lines.
- produce more moment maps and subtraction moment maps for all visible chemical lines in order to test variability using maps more thoroughly.

Both widening the scope and increasing the depth of the analysis of the ALMA data will lead to a greater understanding of high mass star formation and accretion bursts.

Acknowledgements

I would like to thank my supervisor Dr Claudia Cyganowski for enabling me to do this project, and for her guidance throughout the process. Thank you to Rodrigo Hernan Alvarez Gutierrez and David Taylor for all their help and support, and for allowing me to use their python scripts for the data extraction, spectral graphs, and moment maps. Thank you to Sophie Hawkins, my fellow summer student. Finally thank you to Lord Laidlaw and the Laidlaw Foundation for the funding for this research, and to Celina O'Connor for running the Laidlaw Research Programme.

Data availability

The complete set of spectral graphs, moment maps and subtraction moment maps are stored on my personal device, so are available by contacting me via emeline.hulsen@gmail.com. Any questions regarding this article or my work should also be sent this way.

References

[1] T. R. Hunter et al. "An Extraordinary Outburst in the Massive Protostellar System NGC6334I-MM1: Quadrupling of the Millimeter Continuum". In: 837.2, L29 (Mar. 2017), p. L29. DOI: 10.3847/2041-8213/aa5d0e. arXiv: 1701.08637 [astro-ph.SR].

[2] D. M.-A. Meyer et al. "On the existence of accretion-driven bursts in massive star formation". In: *Monthly Notices of the Royal Astronomical Society: Letters* 464.1 (Jan. 2017), pp. L90–L94. ISSN: 1745-3925. DOI: 10.1093/mnrasl/slw187. eprint: https://academic.oup.com/mnrasl/article-pdf/464/1/L90/56943686/mnrasl_464_1_l90.pdf. URL: https://doi.org/10.1093/mnrasl/slw187.

[3] P F Rohde et al. "Protostellar outflows: a window to the past". In: *Monthly Notices of the Royal Astronomical Society* 510.2 (Feb. 2022), pp. 2552–2571. ISSN: 0035-8711. DOI: 10.1093/mnras/stab3572. eprint: https://academic.oup.com/mnras/article-pdf/510/2/2552/42080332/stab3572.pdf. URL: https://doi.org/10.1093/mnras/stab3572.

[4] Á. Sánchez-Monge et al. "ALMAGAL: II. The ALMA evolutionary study of high-mass protocluster formation in the Galaxy: ALMA data processing and pipeline". In: 696, A150 (Apr. 2025), A150. DOI: 10.1051/0004-6361/202452703. arXiv: 2503.05559 [astro-ph.GA].

[5] Yuhan Yang et al. "Tracking Protostellar Variability in Massive Protoclusters with ALMA. I. Insights from QUARKS and MaMMOtH". In: 1003.1, 60 (May 2026), p. 60. DOI: 10.3847/1538-4357/ae5c08. arXiv: 2512.10298 [astro-ph.GA].

[6] Lis Zwicky et al. "Observational chemical signatures of the past FU Ori outbursts". In: 527.3 (Jan. 2024), pp. 7652–7671. DOI: 10.1093/mnras/stad3713. arXiv: 2311.17499 [astro-ph.SR].

Appendices

A Cross-referencing Table

Table 1: Table that compiles information about the peaks in the spectra of every.

Field	Source	Lines in spw 29	Lines in spw 25 (excluding 29)	Lines in spw 31	Lines in spw 27 (excluding 31)
50555	MM1	H2CO(I)	SiS, CH3OH(II), H2CO(III)	CO[13]	CO[18]
	MM2	H2CO(I), CH3OH(III), H2CO(II)	DCN, H2CO	CO[13]	CO[18]
	MM3	—	—	CO[13]	—
53869	MM1	H2CO(I), HC3N, CH3CO(III), H2CO(II)	SiO, DCN, CH3OH(I), either SiS or CH3OH(II), H2CO(III)	CO[13], CH3CN ladder	Combined ONCN and HC3N, CO[18], combined HNCO and CH2CHCN, SO, CH3OH
	MM2	H2CO(I), CH3OH(III), H2CO(II)	DCN, SiS, CH3OH(II), H2CO(III)	CO[13]	CO[18]
	MM3	H2CO(I), HC3N, CH3OH(III), H2CO(II)	DCN, CH3OH(I), SiS, H2CO(III)	CO[13]	CO[18]
56184	MM1	—	—	CO[13]	CO[18]
	MM2	H2CO(I), HC3N	SiS, CH3OH(II)	CO[13]	CO[18], SO
	MM3	H2CO(I)	—	CO[13]	CO[18]
	MM4	—	—	CO[13]	CO[18]
57335	MM1	H2CO(I), HC3N, CH3CO(III), H2CO(II)	DCN, CH3OH(I), CH3OH(II), H2CO(III)	CO[13], CH3CN ladder	HC3N, H2CN, HNCO, SO, CH3OH (many peaks, so identification a little uncertain)
	MM2	H2CO(I), CH3OH(III), H2CO(II)	H2CO(III)	CO[13]	CO[18], SO

	MM3	H2CO(I), CH3OH(III), H2CO(II)	DCN, H2CO(III)	CO[13]	CO[18], SO
58516	MM1	H2CO(I) , HC3N, CH3OH(III) , H2CO(II)	DCN , H2CO(III)	CO[13], weak impressions of a CH3CN ladder	CO[18], SO
	MM2	H2CO(I), CH3OH(III), H2CO(II)	H2CO(III)	CO[13]	CO[18]
	MM3	H2CO(I)	—	CO[13]	CO[18]

Table 1 uses a range of highlighting to indicate variability and other important information, which is explained in Table 2.

Table 2: Key of highlighting used in Table 1.

Component	Highlight
Outburst candidate	(green)
Line rich source	MMx
Variability	(orange)
Possible variability	(light orange)

B Moment Map Summary Table

Table 3: Compilation of information gained from moment maps.

Field	H2CO(I)	HC3N	CH3OH(III)
50555	Locations: Large outflow above and left of MM1, another smaller to the bottom right. One centred on MM2. Two outflows to the bottom left of MM3. Changes: Mar dates are brighter, brightest seems to be 28Mar, also outflows spread out in Mar. Subtraction: Between Dec and Mar, differences around and on MM1. No difference between Mar dates.	No HC3N	Locations: Two outflows above and to the left of MM1. One outflow to the bottom left of MM3. Changes: Mar dates are brighter, brightest seems to be 28Mar. Subtraction: Differences in the outflows between 17Dec and Mar dates. No differences between two Mar dates.
53869	Locations: Centred on MM1. Outflow far to the bottom right of MM1. Large outflow to the left of MM3 Changes: Mar dates seem brighter for MM1 and bottom right outflow. Dec seems brighter for left of MM3 large outflow	Locations: Centred on MM1. Changes: Mar dates seem brighter.	Locations: Centred on MM1. Outflow far to the bottom right of MM1. Large outflow to the left of MM3 Changes: Mar dates seem brighter for MM1 and bottom right outflow Dec seems brighter for left of MM3 large outflow.

Table 3: Compilation of information gained from moment maps.

Field	H2CO(I)	HC3N	CH3OH(III)
	Subtraction: Between Dec and Mar, differences on MM1 and (possibly) outflow to bottom right. No difference between Mar dates.	Subtraction: Between Dec and Mar, differences on MM1. No difference between Mar dates.	Subtraction: Between Dec and Mar, differences on MM1 and outflow to bottom right. No difference between Mar dates.
56184	Locations: Centred on MM2 ans MM3. Some weak smudgy outflows in space between MM1, MM2, and MM3. Possibly some on MM4. Changes: For MM3 and outflows, Mar dates are brighter, but hard to tell otherwise. Subtraction: Overall brightness difference for Dec vs. Mar compared to two Mar dates, but not obvious emission differences.	Locations: Centred on MM2. Very noisy and difficult to see Changes: Dec seems brightest, but 28Mar seems oddly brighter than 29Mar. Subtraction: Overall brightness difference for Dec vs. Mar compared to two Mar dates, but not obvious emission differences.	Can't get a good CH3OH moment map.
57335	Locations: Centred on MM1. Small outflow / smudge to the right of MM2. Changes: Dec brighter than Mar for all. Subtraction: Between Dec and Mar, differences on MM1 and slightly on outflow right of MM2. No difference between Mar dates.	Locations: Centred on MM1. Changes: Dec brighter than Mar. Subtraction: Between Dec and Mar, differences on MM1. No difference between Mar dates.	Locations: Centred on MM1. Small outflow / smudge to the right of MM2. Changes: Dec brighter than Mar for all. Subtraction: Between Dec and Mar, differences on MM1 and slightly on outflow right of MM2. No difference between Mar dates.
58516	Location: Covers MM1, MM2 (and weakly MM3) but does not follow contours. Large outflow above MM1. Changes: Dec brighter than Mar, particularly for outflow. Less MM3 cover in Dec. Subtraction: Between Dec and Mar difference in large outflow above MM1. No difference between Mar dates.	Location: Centred on MM1. Outflow above and slightly right of MM1. Quite noisy. Changes: Dec brighter than Mar for both but particularly outflow. Less noisy in Mar. Subtraction: Seems to be no changes at all, matches with lack on HC3N variability in spectral graphs.	Location: Large outflow above MM1. Some on MM1 and smudgy outflow that covers MM2. Changes: Dec brighter than Mar, particularly for outflow. Subtraction: Between Dec and Mar difference in large outflow above MM1. No difference between Mar dates.

C Fields and Sources

Below are the 5 fields included in this study, and their labelled sources. Sources that have been previously identified as outburst candidates are marked with red.

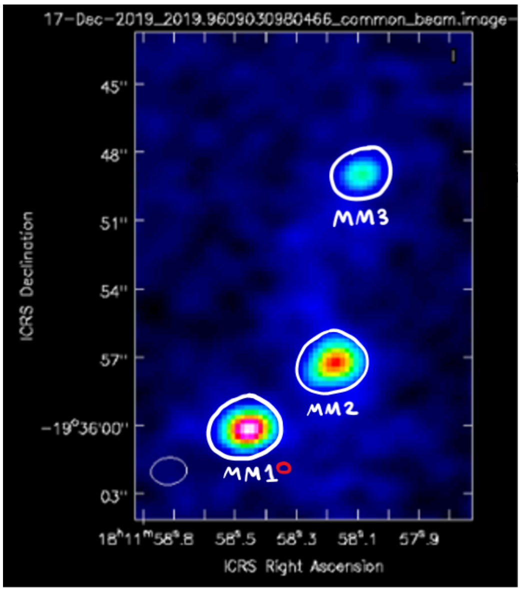

(a) Field 50555

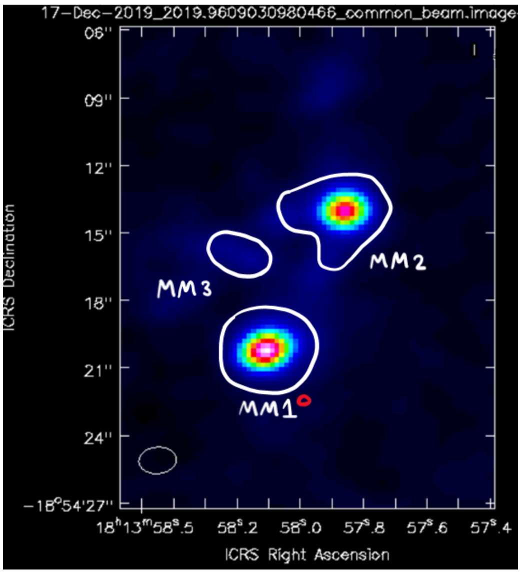

(b) Field 53869

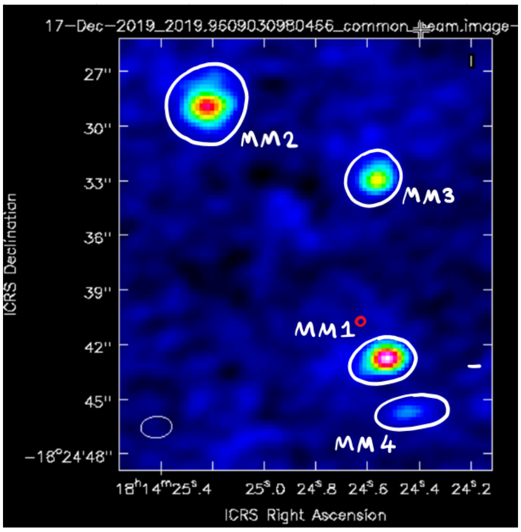

(c) Field 56184

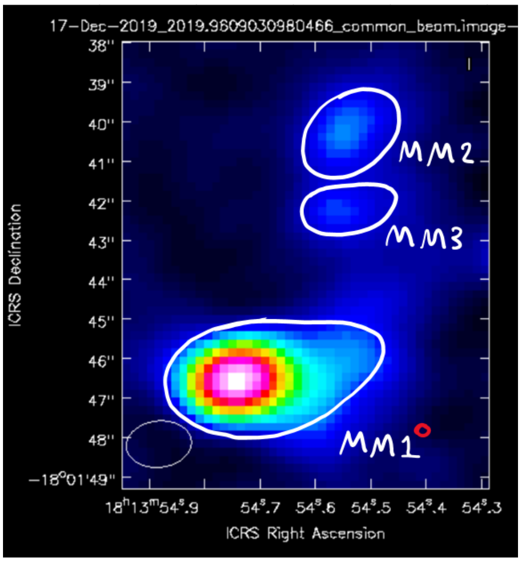

(d) Field 57335

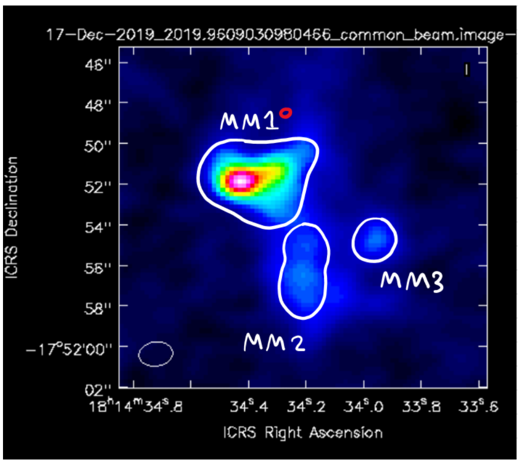

(e) Field 58516